Biological soil crusts as modern analogs for the Archean continental biosphere: insights from carbon and nitrogen isotopes

Christophe Thomazo, Estelle Couradeau, Anna Giraldo-Silva, Johanna Marin-Carbonne, Arnaud Brayard, Martin Homann, Pierre Sans-Jofre, Stefan Lalonde, Ferran Garcia-Pichel

Accepted version of:

BIOLOGICAL SOIL CRUSTS AS MODERN ANALOGUES FOR THE ARCHEAN CONTINENTAL BIOSPHERE: INSIGHTS FROM CARBON AND NITROGEN ISOTOPES

Published in: *Astrobiology* 20, 7, doi.org/10.1089/ast.2019.2144

C. THOMAZO[1,*], E. COURADEAU[2], A. GIRALDO-SILVA[3], J. MARIN-CARBONNE[4], A. BRAYARD[1], M. HOMANN[5,6], P. SANSJOFRE[5,7], S.V. LALONDE[5], F. GARCIA PICHEL[3].

[1] Biogéosciences, UMR6282, CNRS, Université Bourgogne Franche-Comté, 6 Boulevard Gabriel, 21000 Dijon, 0380393578, France (*correspondence: christophe.thomazo@u-bourogne.fr)

[2]Joint Genome Institute, Lawrence Berkeley National lab, Walnut Creek, California, USA

[3] Center for Fundamental and Applied Microbiomics, Biodesign Institute, and School of Life Sciences, Arizona State University, Tempe, Arizona, USA

[4]Institut des Sciences de la Terre, Université de Lausanne, Géopolis Mouline, Lausanne, Suisse

[5]European Institute for Marine Studies, CNRS-UMR6538, Laboratoire Géosciences Océan, Technopôle Brest-Iroise, 29280 Plouzané, France

[6]Department of Earth Sciences, University College London, WC1E 6BS London, UK

[7]MNHN, Sorbonne Université, CNRS UMR 7590, IRD, Institut de Minéralogie, de Physique des Matériaux et de Cosmochimie, Paris, France

Manuscript keywords: isotope biosignature, Early life, Archean, carbon isotope, nitrogen isotope

Abstract

Stable isotope signatures of elements related to life such as carbon and nitrogen can be powerful biomarkers that provide key information on the biological origin of organic remains and their paleoenvironments. Marked advances have been achieved in the last decade in our understanding of the coupled evolution of biological carbon and nitrogen cycling and the chemical evolution of the early Earth thanks in part to isotopic signatures preserved in fossilized microbial mats and organic matter of marine origin. However, the geologic record of the early continental biosphere, as well as its evolution and biosignatures, are still poorly constrained. Following a recent report of direct fossil evidence of life on land at 3.22 Ga, we compare here the carbon and nitrogen isotopic signals of this continental Archean biosphere with biosignatures of cyanobacteria biological soil crusts (cyanoBSCs) colonizing modern arid environments. We report the first extended $\delta^{13}C$ and $\delta^{15}N$ dataset from modern cyanoBSCs and show that these modern communities harbor specific isotopic biosignatures that compare well with continental Archean organic remains. We therefore suggest that cyanoBSCs are likely relevant analogs for the earliest continental ecosystems. As such, they can provide key information on the timing, extent and possibly mechanism of colonization of the early Earth's emergent landmasses.

1. Introduction

During the Archean, the absence of an ozone layer resulted in higher short-wavelength irradiance than today despite the fact that the sun was 30% dimmer (Kasting et al., 1989). Due to

these extreme environmental conditions, Berkner and Marshall (1965) initially hypothesized that the colonization of Earth's emergent landmass would have been impeded until the formation of an ozone shield. However, later findings showed that sulfur vapor and hydrocarbon smog in the primitive ozone-free atmosphere may have strongly attenuated UV radiation (Kasting et al., 1989), and that the Archean landmasses could have been provided sufficient refugia to early photosynthesizers even under high UV fluxes (Garcia-Pichel, 1998). From a theoretical perspective, a continental[*] microbial phototrophic biosphere could have therefore existed early, before the Great Oxidation Event (Beraldi-Campesi et al, 2009; Lalonde and Konhauser, 2015), and have colonized emergent land surfaces (Thomazo et al., 2018).

Today, the strictly microbial terrestrial phototrophic biosphere is dominated by biological soils crusts (BSCs). They represent the Earth's largest biofilm, covering 12% of the continents (Rodriguez-Caballero et al., 2018), typically in areas where plant growth is restricted. While they are composed of a high diversity of microorganisms, they are primarily built by cyanobacteria performing oxygenic photosynthesis (Garcia-Pichel, 2002).

Robust and direct evidence for ancient fossil BSC is found in the 1.2 Ga mid-Proterozoic Apache Supergroup in the Dripping Springs Formation of Arizona (Beraldi-Campesi et al., 2014). Indirect evidence for the presence of an Archean phototrophic biosphere is based on sedimentological observations of paleosols (3.0-3.2 Ga; Retallack et al., 2016) and geochemical arguments suggesting that microorganisms capable of photosynthesis colonized Archean continents prior to the Great Oxidation Event (e.g., Lalonde and Konhauser, 2015; Havig et al., 2019). An early timeline for land colonization, between 3.05 and 2.78 Ga, is also suggested by ancestral state

[*] Continental referring throughout the text to environments experiencing subaerial exposure and desiccation (e.g. fluvial systems, alluvial fans, dryland and playas) associated with strictly terrestrial biosphere and excluding fully aquatic ecosystems (e.g. lakes, ponds and geothermal springs).

reconstruction and relaxed molecular clock analyses of cyanobacterial diversification (Blank and Sanchez-Baracaldo, 2010; Uyeda et al., 2016; Garcia-Pichel et al., 2019).

Two recent pieces of work made significant advances in the early Earth continental biosphere conundrum. Homann et al. (2018) showed that siliciclastic sediments of the 3.22 Ga Moodies Group (South Africa) preserved fossil microbial mats inhabiting continental habitats (i.e. fluvial with periods of terrestrial subaerial exposure and desiccation) and that their coupled carbon isotope compositions of organic matter and bulk nitrogen isotope compositions are statistically different from strictly marine examples preserved elsewhere in the Moodies Group (e.g, Homann et al., 2015). In addition, Thomazo et al. (2018) carried out a meta-analysis of the biogeochemical cycling of nitrogen by the modern terrestrial phototrophic biosphere and highlighted that this ecosystem would have been capable of importing nitrogen gas from the early atmosphere and exporting ammonium and nitrate to the Archean ocean, presumably through fluvial networks. The present contribution fills the gap between these two recent studies by addressing the N and C isotopic signals of modern cyanoBSCs in order to compare their biosignatures with the emerging geochemical continental record of Archean continental life.

2. Materials and Methods

A total of 67 cyanoBSCs samples were collected from different desert areas (supplementary Table 1). They were analyzed for their organic carbon and bulk nitrogen isotope compositions at the Biogéosciences laboratory, Université de Bourgogne, Dijon, France (see supplementary information). Their maturity level (successional stage) was inferred based on visual observations according to the sequence provided by Garcia-Pichel (2002). Only cyanobacteria-dominated BSCs were selected for geochemical analyses since moss and lichen biocrusts are not relevant to the early Earth microbial environment. Although cyanobacteria are always largely dominating the biomass

of early (light) to middle successional stage (dark) BSCs (Chilton et al., 2018), we ran a non-parametric Mann–Whitney U test to determine if lichen-bearing middle stage BSCs (n = 15, supplementary Table 1) bear different C and N isotope distributions. No significant statistical difference was observed in N isotope compositions between early to middle stage cyanoBSCs and middle stage lichen-bearing BSCs (supplementary Fig. 1). However, for C isotope compositions, measured values are statistically different ($p<0.01$) between these two categories. Lichen-bearing BSCs were therefore excluded from our analyses. Early and middle stage cyanoBSCs are statistically identical in their C and N isotope compositions ($p=0.37$ and 0.39, respectively; supplementary Fig. 2).

3. Results

The isotopic signatures of cyanoBSCs show mean values of -22.8 ± 2.3‰ and 3.4 ± 3.5‰ (1σ) for the $\delta^{13}C_{org}$ and $\delta^{15}N_{bulk}$, respectively. With the exception of one study where extreme $\delta^{15}N_{bulk}$ values (in excess of 10‰) were reported in BSCs from Zambia and Botswana (Aranibar et al., 2003), the $\delta^{13}C_{org}$ and $\delta^{15}N_{bulk}$ data available in the literature are consistent with our measurements (supplementary Fig. 3). The C/N atomic ratio shows a mean value of 9.9 ± 1.3, slightly above Redfield. Figure 1 compares observed ranges of $\delta^{13}C$, $\delta^{15}N$ and C/N ratio in our analyses to the main sources of organic matter in continental hydrogeological systems (Finlay and Kendall, 2007), including terrestrial plant detritus and soils (TPDS), macrophytes, benthic algae and cyanobacteria (BAC), and planktonic algae and cyanobacteria (PAC). The isotopic and elementary signatures of cyanoBSCs define a restricted chemical space, partly overlapping the TPDS, BAC and macrophyte data. Based on these isotopic signals, the BSCs and PAC reservoirs are distinguishable (Fig. 1).

Figure 2 compares the $\delta^{13}C_{org}$ and $\delta^{15}N_{bulk}$ signals of the cyanoBSCs measured in this study with the Paleoarchean continental and marine organic remains preserved in the 3.22 Ga old Moodies Group, and to the Paleoarchean marine organic matter reservoir (after Thomazo et al., 2009). The $\delta^{13}C_{org}$ and $\delta^{15}N_{bulk}$ signatures of the cyanoBSCs and marine Moodies Group are statistically different ($p = 0.03$ and 0.07, respectively). However, the isotopic signatures of modern cyanoBSCs are statistically indistinguishable from the continental Moodies Group ($p = 0.25$ and 0.22 for the $\delta^{13}C_{org}$ and $\delta^{15}N_{bulk}$, respectively). Moreover, the Moodies Group continental $\delta^{13}C_{org}$ values bear this characteristic signature at a regional scale and in different time units (Figure 2). Paleoarchean marine isotopic signatures are consistent with reported data for marine mats from the Moodies Group, and significantly different than the cyanoBSCs and the continental mats of the Moodies Group.

4. Discussion

The isotopic biosignatures of cyanoBSCs are different than the PAC reservoir and exhibit a restricted range when compared to the BAC (Fig. 1). In addition to depositional setting information, these new observations can contribute to interdisciplinary sets of data to help make an integrated biosignature assessment in the geological record. In this way, the Figure 2 thus suggests that cyanoBSCs represent modern analogs of communities that colonized Archean continents. This assumption is consistent with studies suggesting that continental colonization by microbial communities may have triggered oxidative weathering on continental surfaces prior to the Great Oxidation Event (e.g., Lalonde and Konhauser, 2015; Havig et al., 2019). Early life on land would have also enhanced the delivery of nutrients to the oceans such as fixed nitrogen (Thomazo et al., 2018) and would have increased the productivity of Paleoarchean shelfs and coastal margin

environments (Lyons et al., 2014). Cyanobacterial land-based modern ecosystems may therefore hold keys in understanding how Earth's early terrestrial biogeochemical cycles were established and how they were linked to biogeochemical cycling in the marine environment.

Modern examples of cyanoBSCs from desert sandy soils are thus likely close analogues for microbial communities that thrived in environments available for the development of an early phototrophic biosphere on Archean continents and rocky planetary surfaces (with reduced clays and carbonates), given the aggressive weathering regime postulated for the early Earth that was largely dominated by siliciclastic inputs (Bose et al., 2012). The Moodies Group hosts the oldest known occurrence of quartz-rich sandstones, locally interbedded with conglomerates, which were deposited in alluvial, fluvial, possibly aeolian, deltaic, tidal, and subtidal paleoenvironments (e.g. Homann et al., 2015). However, given their low preservation potential in the rock record and the multibillion-year geological history of these terrestrial ecosystems, their detection primarily relies on geochemical proxies. As such, indirect evidence based on element mobility patterns in several Archean paleosols have been suggested to speak to the presence of an ancient terrestrial biosphere where organic ligands chelated metals during weathering (Rye and Holland, 2000). We suggest that coupled carbon and nitrogen isotopic signatures of Archean organic remains, associated with their sedimentological contexts, can provide a direct way to robustly backtrack deep time phototrophic life on land in deep time.

5. Conclusions

Using combined C and N isotope biosignatures, we showed here that biological soil crusts represent, among modern microbial ecosystems, a credible analog for one of the oldest archives of continental life on Earth. Moreover, these communities, more widespread at the global scale than hot spring and hydrothermal systems, are thus of prime importance for untangling mechanisms and

consequences of the early Earth land colonization. They also likely contain key information for understanding the evolution of global biogeochemical cycles toward their modern states.

Acknowledgments

This work was supported by the Programme National de Planétologie (PNP) of the CNRS INSU, co-funded by CNES. CT and JMC thanks the European Union's Horizon H2020 research and innovation program ERC (STROMATA, grant agreement 759289).

Author Disclosure Statement

No competing financial interests exist.

References

Aranibar, J. N., Anderson, I. C., Ringrose, S., and Macko, S. A. (2003) Importance of nitrogen fixation in soil crusts of southern African arid ecosystems: acetylene reduction and stable isotope studies. *Journal of Arid Environments* 54: 345-358.

Beraldi-Campesi, H., Farmer J., and Garcia-Pichel, F. (2014) Modern terrestrial sedimentary biostructures and their fossil analogs in Mesoproterozoic subaerial deposits. *PALAIOS* 29: 45-54.

Beraldi-Campesi, H., Hartnett, H., Anbar, A., Gordon, G., and Garcia-Pichel, F. (2009) Effects of biological soil crusts on soil elemental concentrations; implications for biogeochemistry and as traceable biosignatures of ancient life on land. *Geobiology* 7: 348-359.

Berkner, L. V., and Marshall, L. C. (1965) History of major atmospheric components. *Proc. Natl Acad. Sci. USA* 53: 1215–1225.

Blank, C. E., and Sanchez-Baracaldo, P. (2010). Timing of morphological and ecological innovations in the cyanobacteria–a key to understanding the rise in atmospheric oxygen. *Geobiology* 8: 1-23.

Bose, P. K., Eriksson, P. G., Sarkar, S., Wright, D. T., Samanta, P., Mukhopadhyay, S., Mandal, S., Banerjee, S., and Altermann, W. (2012) Sedimentation patterns during the Precambrian: a unique record? *Mar. Pet. Geol.* 33: 34–68.

Chilton, A. M., Neilan, B. A., and Eldridge, D. J. (2018) Biocrust morphology is linked to marked differences in microbial community composition. *Plant and soil* 429: 65-75.

Finlay, J. C., and Kendall, C. (2007) Stable isotope tracing of organic matter sources and food web interactions in watersheds. In *Stable isotopes in ecology and environmental science,* edited by K. Lajtha and R. Michener, Blackwell, pp 283-333.

Garcia-Pichel, F. (1998) Solar Ultraviolet and the evolutionary history of cyanobacteria. *Origins Life Evol. Biosphere* 28: 321-347.

Gamper, A., Heubeck, C., Demske, D., and Hoehse, M. (2012) Composition and microfacies of Archean microbial mats (Moodies Group, ca. 3.22 Ga, South Africa). *Microbial mats in siliciclastic depositional systems through time. SEPM Special Publication* 101: 65-74.

Garcia-Pichel, F. (2002) Desert Environments: Biological Soil Crusts. In *Encyclopedia of Environmental Microbiology,* edited by G. Bitton, John Wiley, New York, pp 1019-1023.

Garcia-Pichel, F., Lombard, T., Soule, T., Wu, S., Dunaj, S., and Wojciechowski, M. F. (2019) Timing the evolutionary advent of cyanobacteria and the later Great Oxidation Event using gene phylogenies of a sunscreen. *mBio* 10: e00561-19.

Havig, J. R., and Hamilton, T. L. (2019) Hypolithic photosynthesis in hydrothermal areas and implications for cryptic oxygen oases on Archean continental surfaces. *Frontiers in Earth Science* 7:15.

Homann, M., Heubeck, C., Airo, A., and Tice, M. M. (2015) Morphological adaptations of 3.22 Ga-old tufted microbial mats to Archean coastal habitats (Moodies Group, Barberton Greenstone Belt, South Africa). *Precambr. Res.* 266: 47–64.

Homann, M., Sansjofre, P., Van Zuilen, M., Heubeck, C., Gong, J., Killingsworth, B., Foster, I. S., Airo, A., Van Kranendong, M. J., Ader, M., and Lalonde, S. V. (2018) Microbial life and biogeochemical cycling on land 3,220 million years ago. *Nature Geoscience* 11: 665.

Kasting, J. F., Zahnle, K. J., Pinto, J. P., and Young, A. T. (1989) Sulfur, ultraviolet radiation and the early evolution of life. *Orig. Life Evol. Biosph.* 19: 95–108.

Lalonde, S. V., and Konhauser, K. O. (2015). Benthic perspective on Earth's oldest evidence for oxygenic photosynthesis. *Proc. Natl Acad. Sci. USA* 112: 995-1000.

Lyons, T. W., Reinhard, C. T., and Planavsky, N. J. (2014). The rise of oxygen in Earth's early ocean and atmosphere. *Nature* 506: 307.

Retallack, G. J., Krinsley, D. H., Fischer, R., Razink, J. J., and Langworthy, K. A. (2016) Archean coastal-plain paleosols and life on land. *Gondwana Research* 40: 1-20.

Rodriguez-Caballero, E., Belnap, J., Büdel, B., Crutzen, P. J., Andreae, M. O., Pöschl, U., and Weber, B. (2018) Dryland photoautotrophic soil surface communities endangered by global change. *Nature Geoscience* 11: 185-189.

Rye, R., and Holland, H. D. (2000) Life associated with a 2.76 Ga ephemeral pond?: evidence from Mount Roe #2 paleosol. *Geology* 28: 483–486.

Thomazo, C., Couradeau, E., and Garcia-Pichel, F. (2018) Possible nitrogen fertilization of the early Earth Ocean by microbial continental ecosystems. *Nat. Com.* 9: 2530.

Thomazo, C., Pinti, D. L., Busigny, V., Ader, M., Hashizume, K., and Philippot, P. (2009). Biological activity and the Earth's surface evolution: insights from carbon, sulfur, nitrogen and iron stable isotopes in the rock record. *Comptes Rendus Palevol* 8: 665-678.

Uyeda, J. C., Harmon, L. J., & Blank, C. E. (2016). A comprehensive study of cyanobacterial morphological and ecological evolutionary dynamics through deep geologic time. *PloS one* 11: 9.

Figures Captions

Figure 1

Typical ranges of $\delta^{13}C$, $\delta^{15}N$ and C/N ratio for the main sources of organic matter in continental hydrogeological systems (modified after Finlay and Kendall, 2007), compared to ranges for cyanobacteria biological soil crusts. TPDS: Terrestrial plant detritus and soils; BAC: benthic algae and cyanobacteria; PAC: planktonic algae and cyanobacteria.

Figure 2

Comparison of the $\delta^{13}C_{org}$ and $\delta^{15}N_{bulk}$ signals of modern analog cyanobacteria biological soil crusts with the Paleoarchean continental and marine organic remains of the Moodies Group (data from unit B of the Dycedale Syncline; Homann et al., 2018 and MdQ1 unit of the Saddleback Syncline; Gamper et al., 2012) and with the Paleoarchean organic matter oceanic reservoir (after Thomazo et al., 2009).

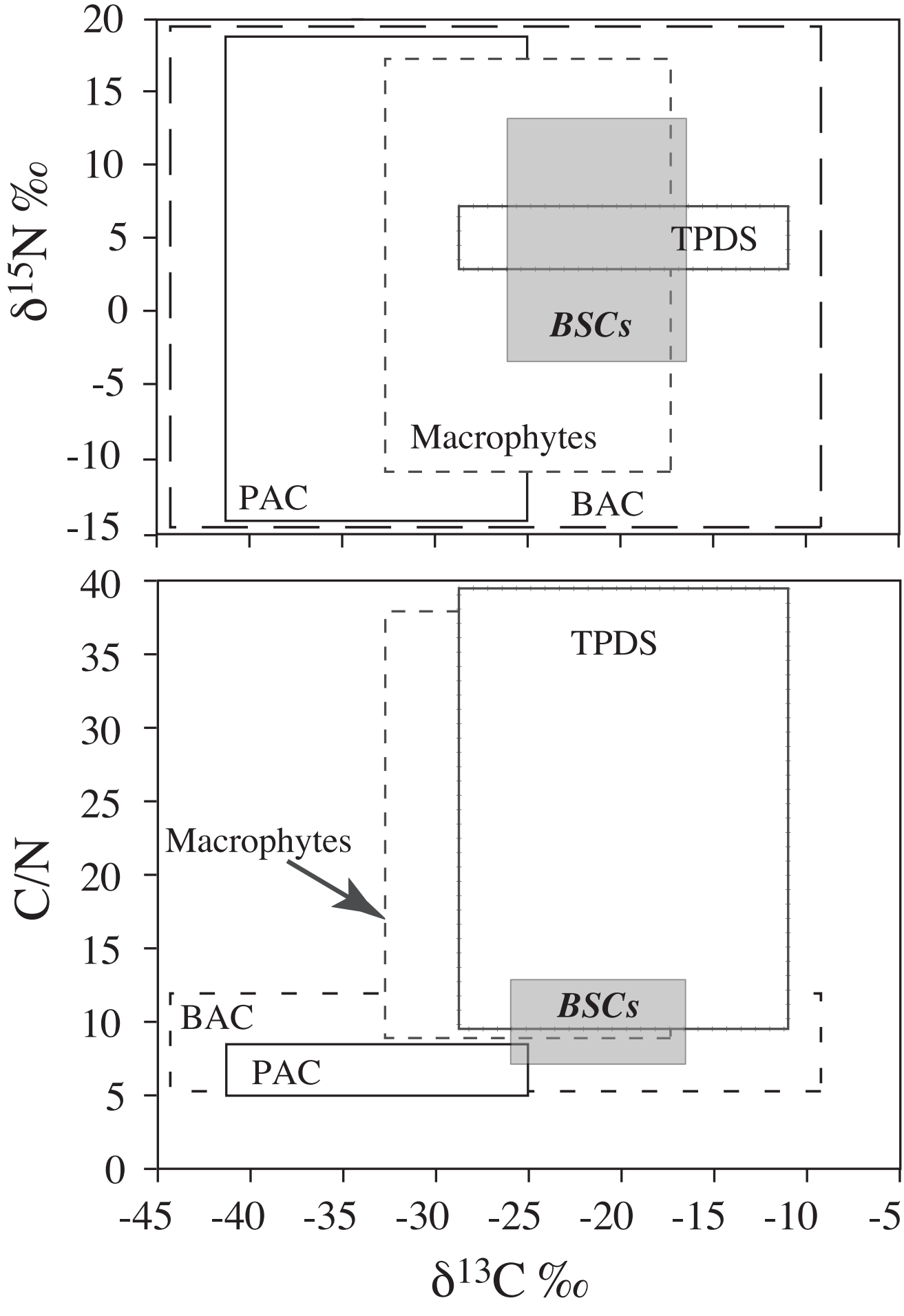
20
15
10
5
0
-5
-10
-15
δ15N ‰
TPDS
BSCs
Macrophytes
PAC
BAC
40
35
30
25
20
15
10
5
0
C/N
TPDS
Macrophytes
BSCs
BAC
PAC
-45
-40
-35
-30
-25
-20
-15
-10
-5
δ13C ‰

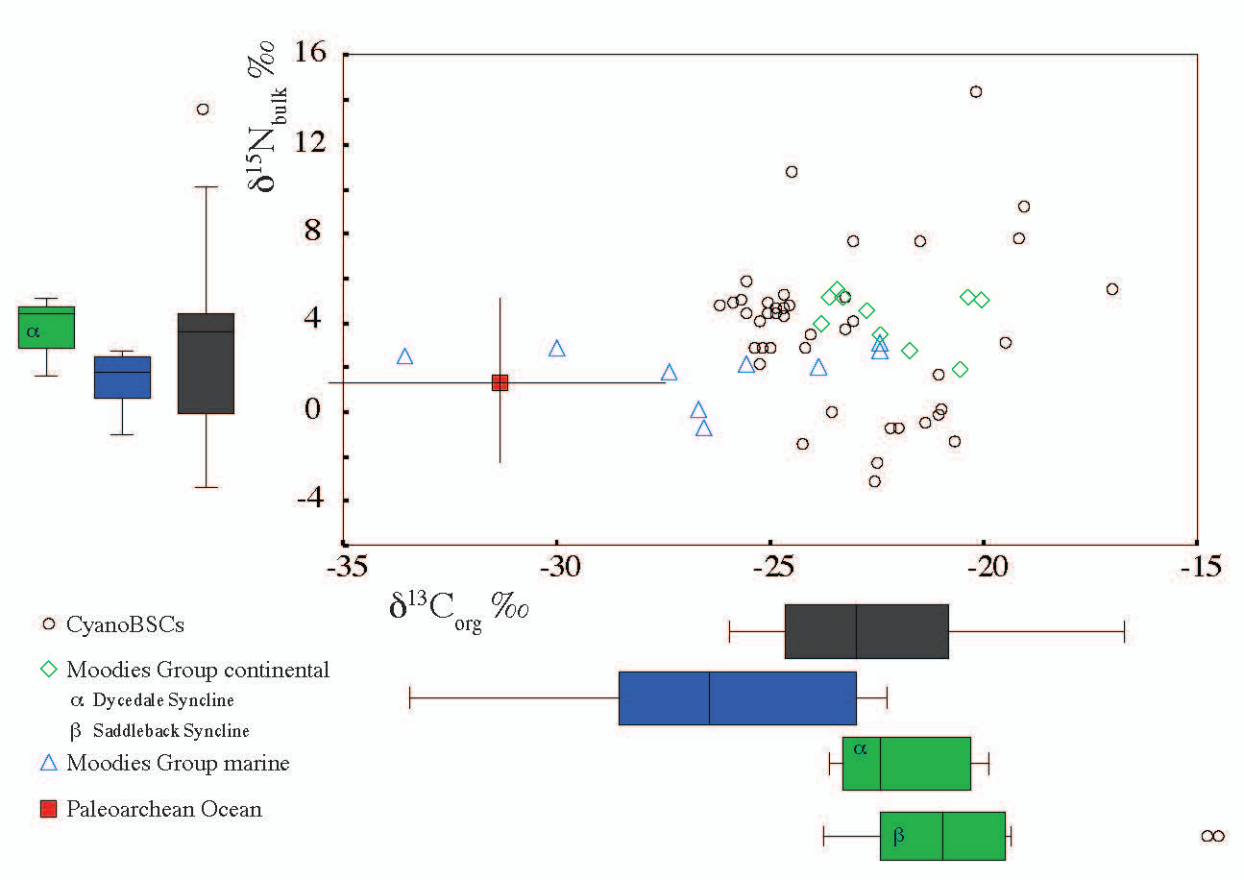
16
12
8
4
0
-4
δ15Nbulk ‰
-35
-30
-25
-20
-15
δ13Corg ‰
α
CyanoBSCs
Moodies Group continental
α Dycedale Syncline
β Saddleback Syncline
Moodies Group marine
Paleoarchean Ocean
α
β
∞

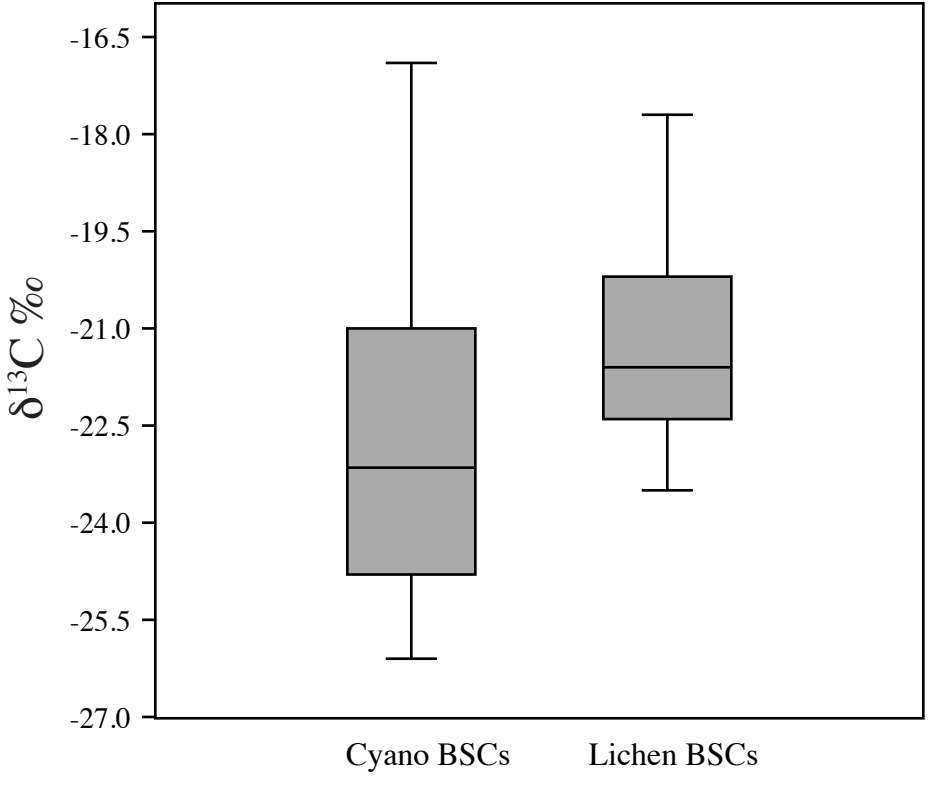
-16.5
-18.0
-19.5
-21.0
-22.5
-24.0
-25.5
-27.0
δ13C ‰
Cyano BSCs
Lichen BSCs

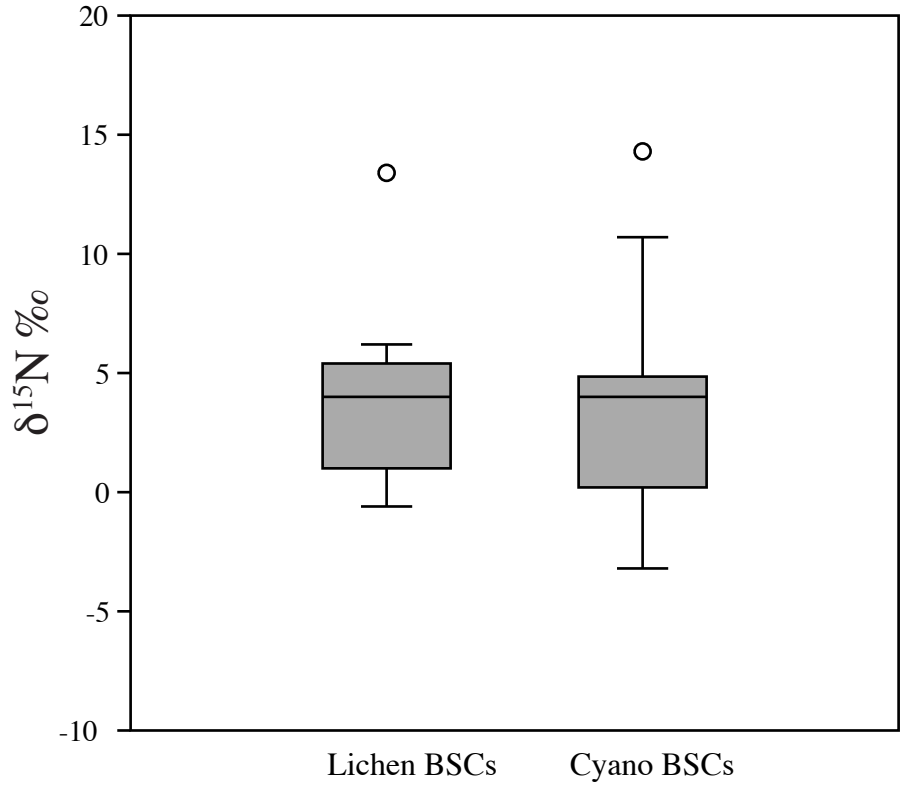
20
15
10
5
0
-5
-10
δ15N ‰
Lichen BSCs
Cyano BSCs

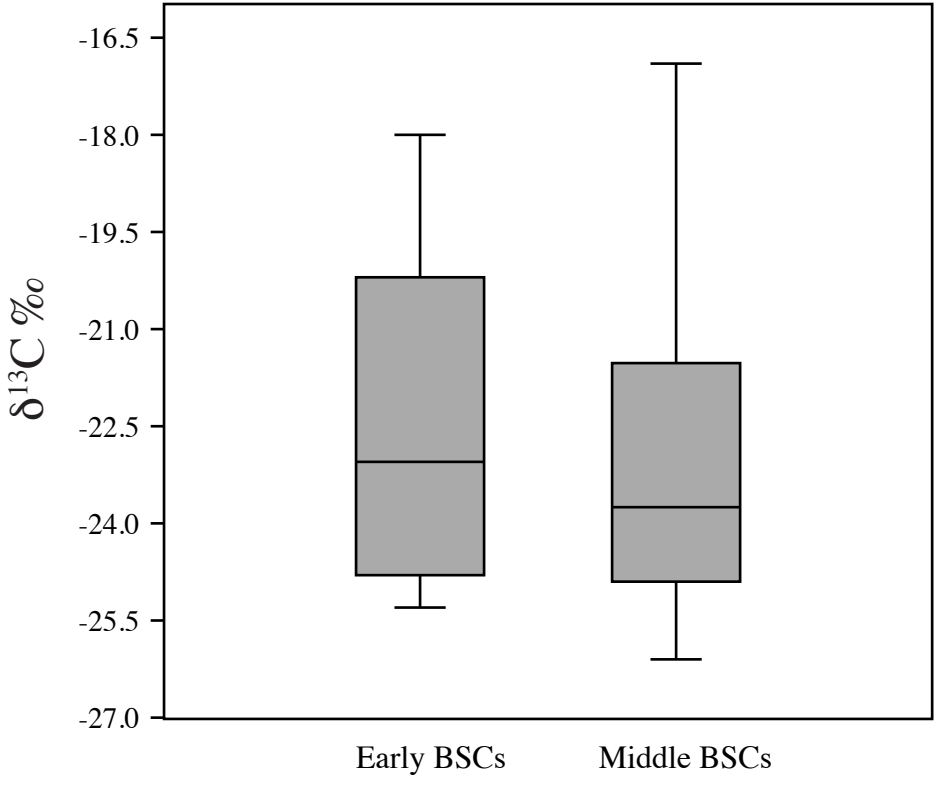
-16.5
-18.0
-19.5
-21.0
-22.5
-24.0
-25.5
-27.0
δ13C ‰
Early BSCs
Middle BSCs

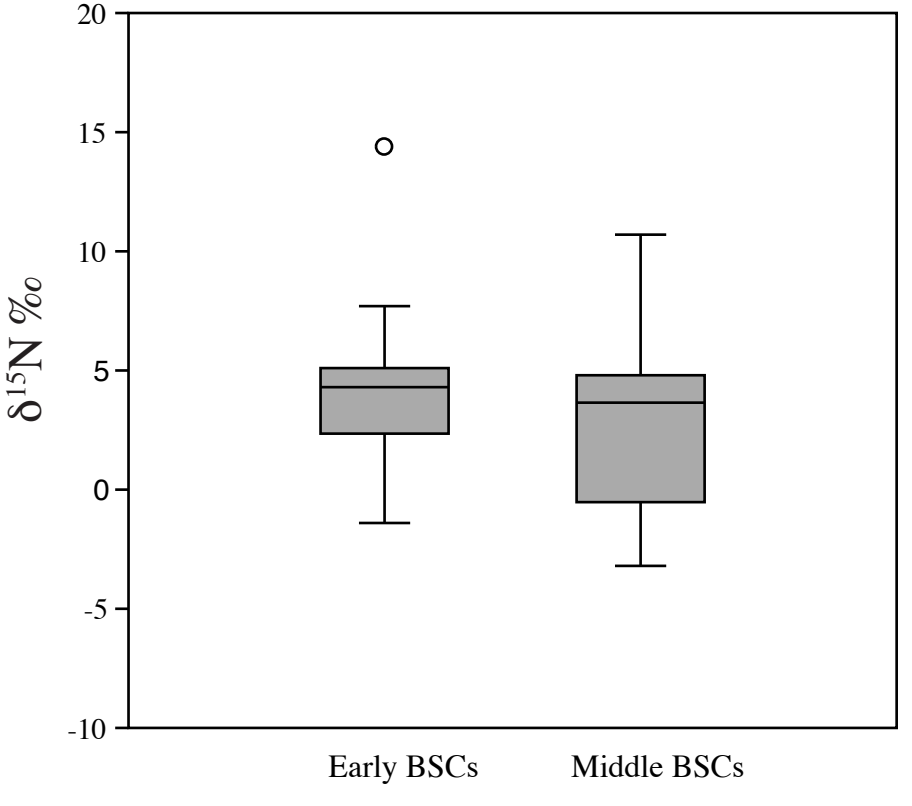
20
15
10
5
0
-5
-10
δ15N ‰
Early BSCs
Middle BSCs

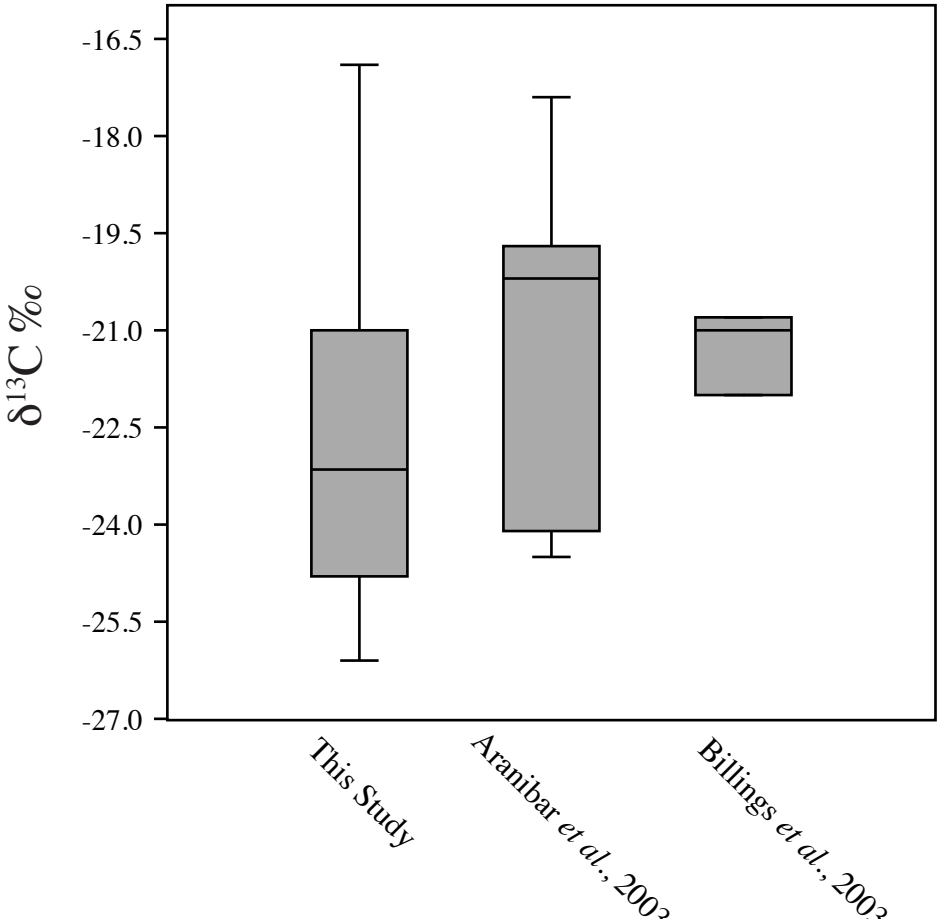
-16.5
-18.0
-19.5
-21.0
-22.5
-24.0
-25.5
-27.0
δ13C ‰
This Study
Aranibar et al., 2003
Billings et al., 2003

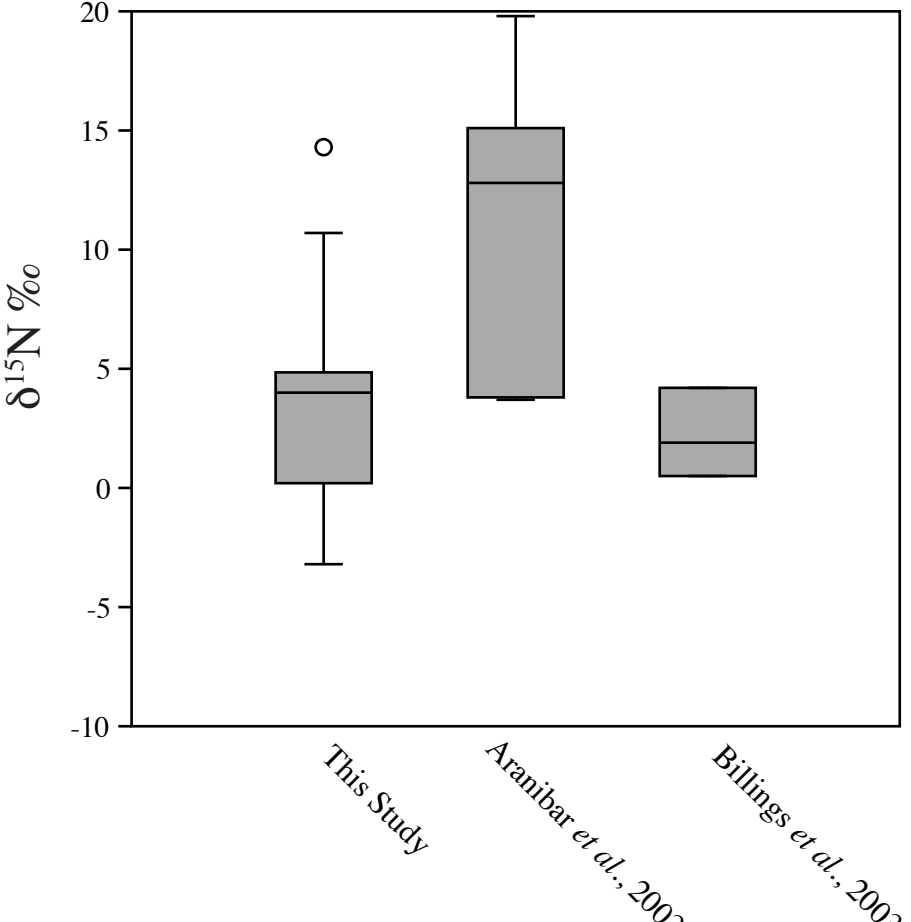
20
15
10
5
0
-5
-10
δ15N ‰
This Study
Aranibar et al., 2003
Billings et al., 2003

Sample ID	Successional stage	Location	GPS coordinates		$\delta^{13}C$ (‰) Vs PDB	$\delta^{15}N$ (‰) Vs AIR	C/N atomic ratio
			Lat	Long			
3FBCYA	Early	Chihuahuan Desert - Fort Bliss air force	32° 25' 51.85"N	105° 59' 2.94"W	-19.8	N.D.	N.D.
5GB	Early	Moab, UT	38° 42' 57.7"N	109° 41' 31.1"W	-19.3	N.D.	N.D.
6GB1097	Early	Moab, UT	38° 42' 57.7"N	109° 41' 31.1"W	-18	N.D.	N.D.
19Arches	Early	Arches National Park, UT	38° 43' 30.61"N	109° 36' 33.39"W	-23	0.4	10
20UT	Early	Moab, UT	38° 34' 58.7"N	109° 31' 27.2"W	-22	N.D.	N.D.
21DM	Early	Moab, UT	38° 34' 58.7"N	109° 31' 27.2"W	-23.1	N.D.	N.D.
23Green	Early	Moab, UT	38° 42' 57.7"N	109° 41' 31.1"W	-18.7	N.D.	N.D.
26MO	Early	Mojave desert, Arizona	35° 15' 11.4"N	115° 58' 38"W	-20.5	N.D.	N.D.
31	Early	Chihuahuan Desert - Fort Bliss air force	32° 25' 51.85"N	105° 59' 2.94"W	-23.2	5	9.8
UNK	Early	Great Basin Desert, UT	41° 6' 15.16"N	113° 0' 29.53"W	-19.1	7.7	9.3
35	Early	Desert Botanical Garden, Phoenix	33° 27' 49.29"N	111° 56' 40.75"W	-24.8	4.3	9.3
36	Early	Desert Botanical Garden, Phoenix	33° 27' 49.29"N	111° 56' 40.75"W	-25.1	2.7	9.5
37	Early	Desert Botanical Garden, Phoenix	33° 27' 49.29"N	111° 56' 40.75"W	-24.5	4.7	9.1
38	Early	Desert Botanical Garden, Phoenix	33° 27' 49.29"N	111° 56' 40.75"W	-25.2	2	9.9
39	Early	Desert Botanical Garden, Phoenix	33° 27' 49.29"N	111° 56' 40.75"W	-25	4.3	10.1

40	Early	Desert Botanical Garden, Phoenix	33° 27' 49.29"N	111° 56' 40.75"W	-24.9	2.8	10.1
41	Early	Desert Botanical Garden, Phoenix	33° 27' 49.29"N	111° 56' 40.75"W	-25.3	2.7	11.0
42	Early	Desert Botanical Garden, Phoenix	33° 27' 49.29"N	111° 56' 40.75"W	-24.8	4.6	8.6
DBG2	Early	Desert Botanical Garden, Phoenix	33° 27' 47.41"N	111° 56' 47.43"W	-24.6	5.2	11.6
XBU	Early	Xiaobing hill, UT	38° 42' 58.7"N	109° 41' 33.7"W	-20.1	14.3	9.0
GREEN	Early	Dinosaure Mountain, Moab, UT	38° 42' 58.7"N	109° 41' 33.7"W	-21	1.5	10.1
DINO	Early	Dinosaure Mountain, Moab, UT	38° 42' 58.7"N	109° 41' 33.7"W	-23.2	3.6	7.1
CASA	Early	Casa Grande, Arizona	32° 59’ 28.9” N	111° 45’ 40.6” W	-23	7.5	6.9
Moabs1L	Early	Moab, UT	38° 42' 58.7"N	109° 41' 33.7"W	-20.6	-1.4	8.1
SUN	Middle	Sunday Churt, UT	38° 38’N	109° 39’W	-21.9	-0.9	10.2
17SM	Middle	Peralta trail, Supertition mountains, Phoenix	33° 14' 18.89"N	111° 12' 31.43"W	-23.5	-0.1	9.7
18Moab	Middle	Moab, UT	38° 42' 58.7"N	109° 31' 27.2"W	-24.2	-1.6	11.0
22Cactus	Middle	Mojave desert, Arizona	34° 07' 49.6"N	114° 14' 28.5"W	-20.9	0	9.2
25Chandler	Middle	Chandler, Arizona	33° 15' 21.8"N	111° 56' 29.5"W	-24.4	10.7	8.4
32	Middle	Great Basin Desert, UT	41° 6' 15.16"N	113° 1' 23.49"W	-23	4	10.9
33	Middle	Moab, UT	38° 38' 6.36"N	109° 38' 9.19"W	-21.3	-0.6	10.8
43	Middle	Desert Botanical Garden, Phoenix	33° 27' 49.29"N	111° 56' 40.75"W	-25.2	4	10.9

44	Middle	Desert Botanical Garden, Phoenix	33° 27' 49.29"N	111° 56' 40.75"W	-24.6	4.2	11.2
45	Middle	Desert Botanical Garden, Phoenix	33° 27' 49.29"N	111° 56' 40.75"W	-25.5	5.7	10.3
46	Middle	Desert Botanical Garden, Phoenix	33° 27' 49.29"N	111° 56' 40.75"W	-25.5	4.3	11.7
47	Middle	Desert Botanical Garden, Phoenix	33° 27' 49.29"N	111° 56' 40.75"W	-25.6	4.9	10.8
48	Middle	Desert Botanical Garden, Phoenix	33° 27' 49.29"N	111° 56' 40.75"W	-24.6	4.6	11.7
49	Middle	Desert Botanical Garden, Phoenix	33° 27' 49.29"N	111° 56' 40.75"W	-25	4.8	10.9
50	Middle	Desert Botanical Garden, Phoenix	33° 27' 49.29"N	111° 56' 40.75"W	-26.1	4.7	12.1
DBG1	Middle	Desert Botanical Garden, Phoenix	33° 27' 47.41"N	111° 56' 47.43"W	-24	3.3	9.1
DBG4	Middle	Desert Botanical Garden, Phoenix	33° 27' 47.41"N	111° 56' 47.43"W	-24	3.3	10.3
DBG5	Middle	Desert Botanical Garden, Phoenix	33° 27' 47.41"N	111° 56' 47.43"W	-25.8	4.8	12.4
DBG7	Middle	Desert Botanical Garden, Phoenix	33° 27' 47.41"N	111° 56' 47.43"W	-24.1	2.8	7.1
Moabsd	Middle	Great Basin Desert, UT	38° 42' 58.7"N	109° 41' 33.7"W	-22.4	-2.4	9.0
Moabs1dk	Middle	Great Basin Desert, UT	38° 42' 58.7"N	109° 41' 33.7"W	-22.5	-3.2	9.4
7GB1084	Middle	Moab, UT	38° 39' 22"N	109° 39' 14.4"W	-21	-0.3	11.0
8GB1014	Middle	Moab, UT	38° 39' 22"N	109° 39' 14.4"W	-21.9	-0.9	11.7

10FB2013	Middle	Chihuahuan Desert - Fort Bliss air force	32° 25' 51.85"N	105° 59' 2.94"W	-19.4	3	9.5
12HSI5	Middle	Great Basin Desert, UT	41° 6' 15.16"N	113° 0' 29.53"W	-19	9.1	9.3
13HSA5	Middle	Great Basin Desert, UT	41° 6' 15.16"N	113° 0' 29.53"W	-16.9	5.4	9.3
16PT	Middle	Peralta trail, Supertition mountains, Phoenix	33° 14' 18.89"N	111° 12' 31.43"W	-22.1	-0.9	9.1
27CH	Middle	Chandler, Arizona	33° 15' 21.8"N	111° 56' 29.5"W	-21.4	7.6	9.5
1HSN	Middle-Lichens	Great Basin Desert, UT	41° 6' 15.2"N	113° 1' 23.50"W	-18.3	6.2	10.3
2HS	Middle-Lichens	Great Basin Desert, UT	41° 6' 15.2"N	113° 1' 23.50"W	-21.9	4	9.1
4HSBCYA	Middle-Lichens	Great Basin Desert, UT	41° 6' 15.2"N	113° 1' 23.50"W	-21.6	5.4	9.9
9NM17	Middle-Lichens	Cibola National Forest, New Mexico	35° 12' 13.33"N	106° 28' 22.98"W	-21.1	1	12.1
11A2013	Middle-Lichens	A mountain, Las Curces, New Mexico	32° 17' 55.97"N	106° 42' 5.15"W	-21.4	5.3	9.5
17Taylor	Middle-Lichens	Jornada LTER, New Mexico	32° 17' 55.97"N	106° 42' 5.15"W	-18.5	2.1	9.1
15CG	Middle-Lichens	Casa Grande, Arizona	32° 59’ 28.9”N	111° 45’ 40.6”W	-22.9	4.1	6.9
24San	Middle-Lichens	Sonoran, Arizona	32° 45’ 2.3”N	113° 39’ 19.0”W	-17.7	13.4	10.0
29	Middle-Lichens	A mountain, Las Curces, New Mexico	32° 17' 55.97"N	106° 42' 5.15"W	-22.6	2.8	9.4
30X1	Middle-Lichens	Great Basin Desert, UT	41° 6' 15.16"N	113° 0' 29.53"W	-22.3	5.3	9.5

DBG3	Middle-Lichens	Desert Botanical Garden, Phoenix	33° 27' 47.41"N	111° 56' 47.43"W	-23.5	0.8	9.4
XBC	Middle-Lichens	Xiaobing chihuahua, New Mexico	32° 32' 60"N	106° 43' 12"W	-20.9	0.6	9.4
XBH	Middle-Lichens	Xiaobing hill, UT	41° 6' 0"N	113° 0' 0"W	-22.4	5.6	9.7
CIBOLE	Middle-Lichens	Cibola National Forest, New Mexico	34° 12' 25.9"N	107° 55' 22.1"W	-20.2	1.1	11.4
Moab-S3	Middle-Lichens	Great Basin Desert, UT	38° 42' 58.7"N	109° 41' 33.7"W	-22.3	-0.6	10.3

*N.D. non-determined - below detection limit